Role of Ti in direct active bonding of SiC substrate using Sn–Ag–Ti alloy filler

L. X. Cheng[1,*] , K. B. Ma[2], X. J. Yue[1], Z. L. Li[3], and G. Y. Li[4]

[1] College of Electronic Engineering, South China Agricultural University, Wushan R. D., Tianhe District, Guangzhou 510642, China

[2] China Electronic Product Reliability and Environmental Testing Research Institute, Dongguanzhuang R. D., Tianhe District, Guangzhou 510610, China

[3] School of Preclinical Medicine, Zunyi Medical University Zhuhai Campus, Jinwan R. D., Jinwan District, Zhuhai 519041, China

[4] School of Electronic and Information Engineering, South China University of Technology, Wushan R. D., Tianhe District, Guangzhou 510641, China

ABSTRACT

Low-temperature active bonding of silicon carbide substrate using Sn3.5Ag4-Ti(Ce,Ga) active solder filler was carried out at 250 °C and 420 °C in air, respectively. The microstructure of the interface, the element distribution, and the new compounds formed at the interface had been investigated. The obvious segregation of titanium at the silicon carbide (SiC)/Sn3.5Ag4Ti(Ce,Ga) interface was observed for both soldering temperatures, in which the segregation rate at 420 °C is faster than that at 250 °C, because the diffusion coefficient of Ti is an exponential function of temperature. Results of transmission electron microscope analysis show that the reactants at the interface of SiC/Sn3.5Ag5Ti(Ce,Ga) of the joint soldered at 250 °C for 60 min were not observed although the segregation of Ti existed at the boundary. However, the TiC, Ti_5Si_3, and $TiSi_2$ were found to be discontinuously formed at the interface for the joints soldered at 420 °C for 30 min. The work of adhesion of Ti on the surface of SiC is calculated, which might be inferred that the joining could be accomplished by chemical adsorption of titanium at the SiC/Sn3.5Ag4Ti(Ce,Ga) interface, regardless of whether an interfacial reaction layer is formed or not. The shear strength of the joints soldered at 420 °C is higher than that at 250 °C. This indicates that the formation of the reaction products plays a critical role to obtain more reliable bond between SiC and Sn3.5Ag4Ti(Ce,Ga), although it is not a necessary condition to realize bonding with reasonable strength.

Address correspondence to E-mail: chenglx@scau.edu.cn

Springer

1 Introduction

Silicon carbide (SiC), the third-generation semiconductor material, is a kind of ceramics in a broad sense, which is hard and brittle and has low toughness and ductility, high melting point, and high chemical stability [1, 2]. Due to its small lattice mismatch, low dislocation density, and good thermal conductivity, SiC is very suitable for the growth of high-quality Gallium nitride (GaN) epitaxial materials [3] and becomes the main substrate material for high-frequency and high-power GaN high electron mobility transistor (HEMT) devices [4, 5]. However, before pre-metallization, SiC cannot be soldered with traditional solder, which leads to the need of high-temperature treatment and chemical reaction in the substrate-packaging process of GaN devices with SiC substrate.

By summarizing and analyzing the previous research results, it is clear that the direct bonding of SiC can be realized by using the active solder doped with active element Ti [6, 7]. However, the research on SiC active welding is mainly concentrated on the field of high temperature [8–10], and the research on low temperature is less. Especially for the low-temperature active SnAgTi solder, only B. Z. Wu, W. Y. Yu and L. C. Tsao etc. conducted research on it in recent years. Wu [11] took ultrafast air bonding on SiC ceramic using SnAgTi alloy under the action of ultrasounds. The effects and mechanism of ultrasonic action on the interfacial bonding and microstructure were investigated. Yu only performed tests on the spreading of SnAgTi solder droplets on the surface of porous graphite through ultrasonic vibration [12]. Tsao analyzed the distributions of alloy elements at the interface in direct active soldering of $Al_{0.3}Cr$ $Fe_{1.5}Mn$ $Ni_{0.5}$ high-entropy alloy to 6061-Al using SnAgTi active solder, and the microstructures of the interface were not deeply analyzed [13]. The kinetic processes of diffusion, adsorption, and interface reaction of active elements at low-temperature active welding were rarely analyzed, and there was no unified understanding as well. Therefore, it is very necessary to actively carry out in-depth research and analysis on the low-temperature soldering SiC using SnAgTi filler alloy. In addition, Mishra et al. [14] pointed out in a review paper that interface reaction was inevitable in most metal–ceramic soldering. Liquid metals did not wet the ceramic substrate unless there was a reaction between the corresponding ceramic–metal interfaces which increased the wetting of the liquid metal. However, Chung [15], Gremillard [16], and Rado [17] delivered that whether or not reactive phase was formed at the bonding interface, the joint could be realized by the chemical adsorption of Ti at the interface. This signified that it had not been fully confirmed that if the formation of compounds at the bonding interface was a necessary condition for the connection between ceramic and active solder.

To well understand the soldering mechanisms of low-temperature active solder SnAgTi with SiC, and to explore whether the formation of new compounds is a necessary condition for the interfacial connection, this paper carried out the research on the low-temperature active bonding of SiC using SnAgTi solder filler at two different bonding temperatures. The microstructures of the interface, the element distributions, and the new compounds formed at the interface had been investigated in this study. The bonding strength of two group samples prepared at different bonding temperatures was measured, and the influence of bonding temperature on mechanical properties was also discussed.

2 Experimental

The SnAgTi filler alloy used in the study was provided by S-BOND Technologies. The solidus and liquidus temperatures are 221 °C and 232 °C, respectively. The 4H-SiC substrate for bonding was supplied by Harbin Tebo Technology Co., Ltd. Prior to soldering, SiC wafers were all finely polished and cleaned. The samples were prepared in the same way as we used in our previous studies [18], in which two
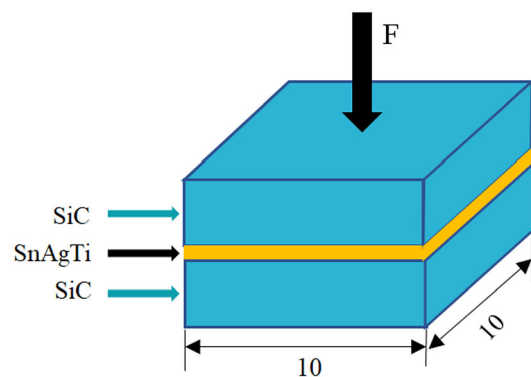

Fig. 1 Schematic representation of soldering (Units: mm)

pieces of SiC were bonded together to form a sandwich structure, as shown in Fig. 1. In order to compare and analyze the influence of bonding temperature on the joint interface, two bonding temperatures were set to be 250 °C and 420 °C, respectively. The cross-sections of the samples were prepared by traditional metallographic method for metallographic observation. The joint interface micromorphology and elements distribution were observed by a scanning electron microscopy (SEM: HITACHI S-3700N) coupled with energy dispersive spectrometer (EDS). A field emission transmission electron microscopy (TEM: JEM-2100F) was used to further identify the interfacial compounds and the microstructures. The shear strength of SiC/SnAgTi/SiC joints was gauged by a bond tester (MFM1500) according to the test method of chip bonding shear strength in MIL-STD-883G-2006, and the shear speed was set to be 300 μm/s. There were ten samples in each group for the shear strength testing, and the average value was taken as the final test result.

3 Experimental results

3.1 Characterization of solder material

SEM microstructure of the Sn3.5Ag4Ti(Ce,Ga) active solder is shown in Fig. 2, and the EDS analysis for different phases indicated in Fig. 2 is shown in Table 1. Results show that the Sn3.5Ag4Ti(Ce,Ga) active solder mainly consists of the Sn matrix (A1), small white of Ag_3Sn phase (A2), grayish white Sn_3Ti_2 phase (A3), and gray Sn_5Ti_6 phase (A4). Figure 3
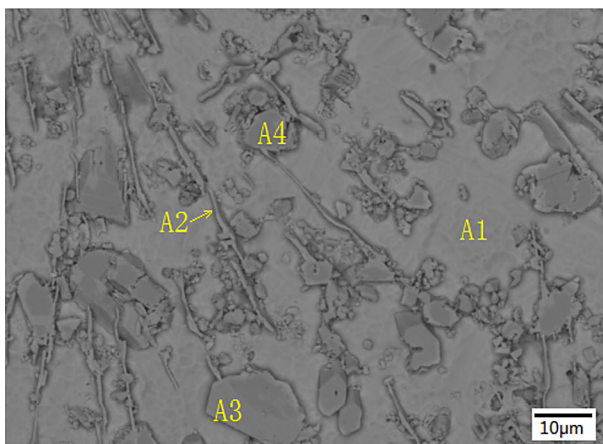

Fig. 2 SEM microstructure of the Sn3.5Ag4Ti(Ce,Ga) active solder

Table 1 Average chemical compositions of each phase on the Sn3.5Ag4Ti(Ce,Ga) active solder

Site	Average chemical composition (at.%)			Phase
	Sn	Ag	Ti	
A1	99.53	0.47	–	Sn
A2	26.31	73.69	–	Ag_3Sn
A3	58.75	–	41.25	Sn_3Ti_2
A4	42.16	–	57.84	Sn_5Ti_6

illustrates the X-ray diffraction pattern of the Sn3.5Ag4Ti(Ce,Ga) active solder. It is further confirmed that the Sn, Ag_3Sn, Sn_5Ti_6, and Sn_3Ti_2 phases exist in the solder.

It can be found that there are both Sn–Ti and Sn–Ag clusters existing in the solder. However, before adding the element titanium, Sn3.5Ag is a eutectic solder with a melting point of 221 °C. The microstructure is mainly composed of Sn and Ag_3Sn phases. The Sn–Ti phase appears only after the addition of titanium. According to the character of the elements in the alloy, when at the liquid state, the dissolution enthalpy of Ti in Sn (− 74 kJ/mol) is far lower than the dissolution enthalpy of Ag in Sn (− 10 kJ/mol) [19]. Therefore, the combining ability of Sn–Ti is much stronger than that of Sn–Ag. So the addition of titanium may slightly increase the liquidus temperature of the bonded solder.

3.2 Elemental distribution

The interface micrograph in backscattered electron (BSE) mode and the corresponding elemental distribution of the SiC/Sn3.5Ag4Ti(Ce,Ga)/SiC joint soldered at 250 °C for 1 min are shown in Fig. 4. It can be seen clearly from the figure that titanium element forms agglomeration inside the active solder, which is basically consistent with the microstructure of the solder itself. And tin and silver elements are evenly distributed in the solder. No obvious segregation of titanium was observed at the SiC/active solder interface, and there was also no visible and recognizable compound observed at the interface either. The element maps of tin, titanium, and silver are shown in Fig. 4b–d, respectively.

The interface micrograph and the corresponding element maps for SiC/Sn3.5Ag4Ti(Ce,Ga)/SiC joint soldered at 250 °C for 30 min are shown in Fig. 5.

Fig. 3 X-ray diffraction spectra of the Sn3.5Ag4Ti(Ce,Ga) active solder
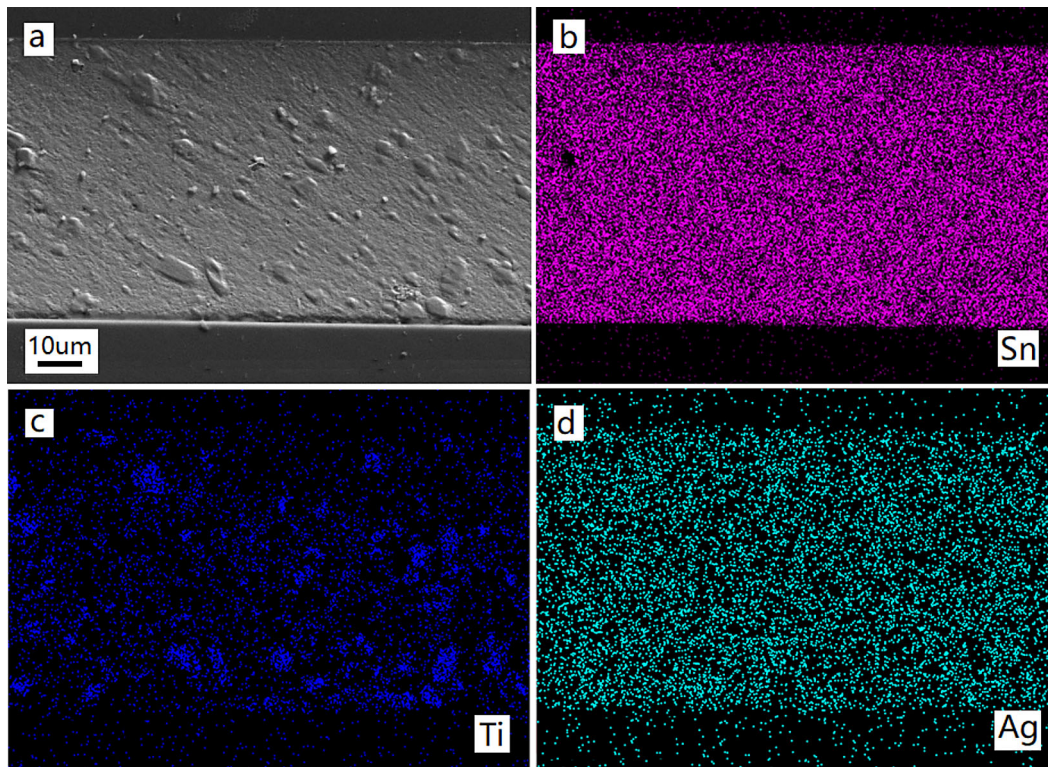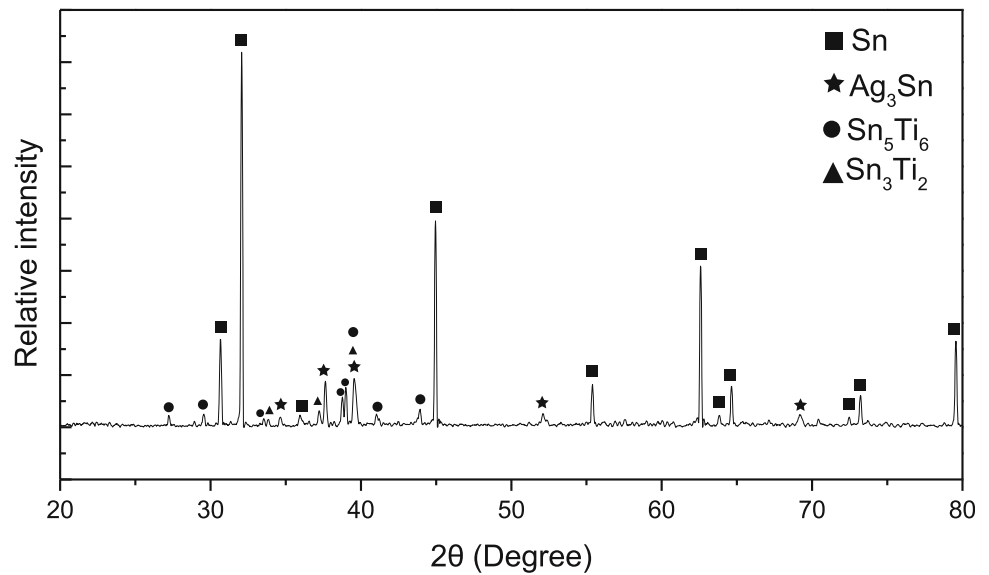

Fig. 4 Micrograph and element maps for SiC/SnAgTi/SiC joint soldered at 250 °C for 1 min. **a** micrograph; **b** map of tin; **c** map of titanium; and **d** map of silver

Comparing Fig. 5c with Fig. 4c, it can be found that the amount of titanium elements agglomerated inside the active solder after soldering is significantly reduced. There is no change in the distribution of tin and silver, which are also evenly distributed in the active solder. Moreover, no obvious segregation of titanium was found at the SiC/SnAgTi joint interface.

The interface micrograph and the corresponding element maps for SiC/Sn3.5Ag4Ti(Ce,Ga)/SiC joint soldered at 250 °C for 60 min are shown in Fig. 6. As you can see in Fig. 6 a, there is still no visible
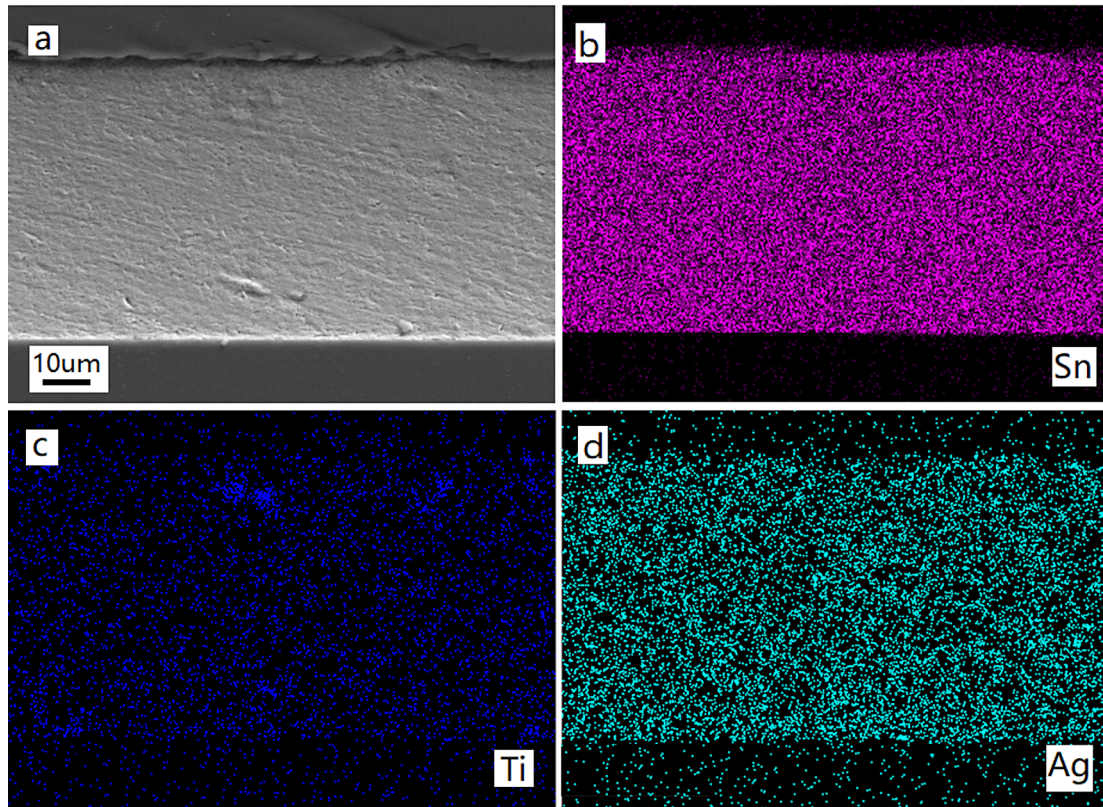
Fig. 5 Micrograph and element maps for SiC/SnAgTi joint soldered at 250 °C for 30 min. **a** micrograph; **b** map of tin; **c** map of titanium; **and d** map of silver

compound layer found to be formed at the interface. However, the obvious segregation of titanium elements can be observed at the soldering interface, as shown in Fig. 6c, and the most Ti agglomeration appeared inside the solder before it disappears. It can be observed from Figs. 4c and 5c that titanium element gradually evolves from agglomeration inside the solder to segregation at the joint interface with the increasing in soldering time.

In order to analyze the influence of soldering temperature on the element distribution of solder alloy during bonding process, SEM micrograph and element maps for SiC/SnAgTi/SiC joints soldered at 420 °C with different holding time were obtained. Figure 7 shows micrographs and element maps for SiC/SnAgTi/SiC joint soldered at 420 °C for 1 min. From these figures, you can see that titanium element still forms agglomeration inside the active solder after soldering. No obvious segregation of titanium was found at the SiC/active solder interface, which was almost the same as that soldered at 250 °C with 1 min.

Micrograph and element maps for SiC/SnAgTi/SiC joint soldered at 420 °C for 30 min are shown in Fig. 8. It can be seen from Fig. 8c that the titanium element has obviously segregated at the soldering interface between SiC and SnAgTi, which is very different from that soldered at 250 °C with 30 min. This means that the time required for titanium element to segregate at the soldering interface is not all the same for different soldering temperatures. To understand how the bonding temperature and time affect the Ti diffusion and segregation in soldering processes, further investigation needs to be carried out.

To investigate the behavior of active element titanium under the extension of holding time, micrograph and element maps for SiC/SnAgTi/SiC joint soldered at 420 °C for 60 min were taken concurrently, as shown in Fig. 9. From Fig. 9c, it can be seen that more active element Ti is segregated at the interface and presenting a wider continuous line shape. This might indicate that the active element titanium is firmly adsorbed on the bonding interface, or a slice of new phases containing titanium element
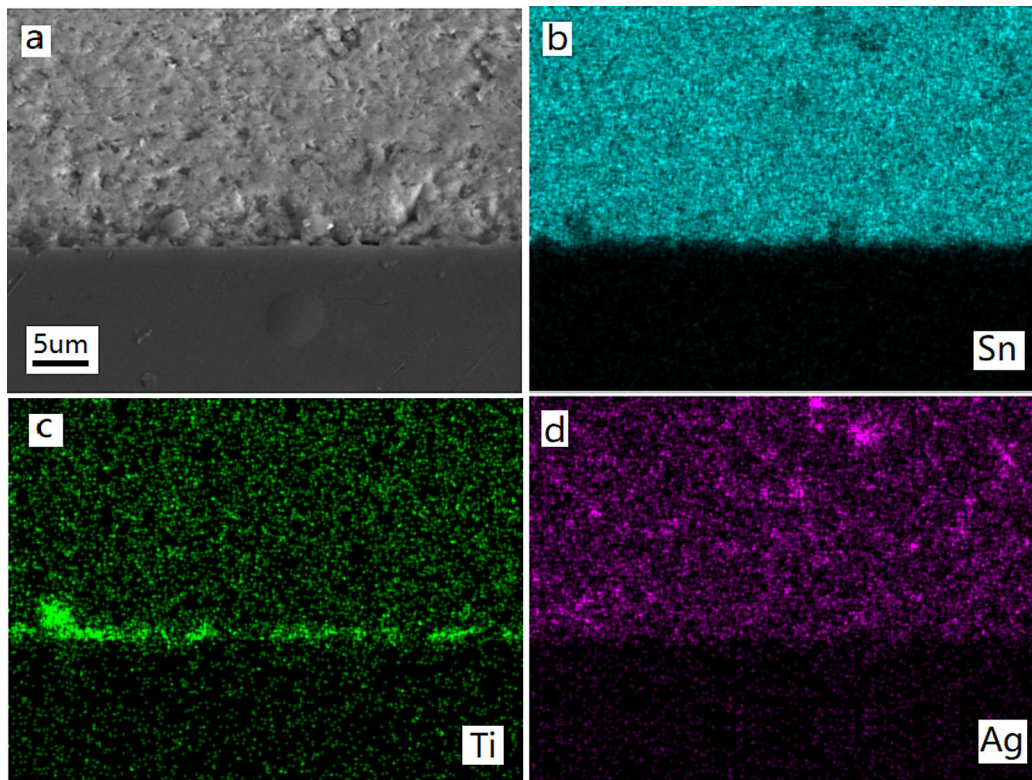
Fig. 6 Micrograph and element maps for SiC/SnAgTi joint soldered at 250 °C for 60 min. **a** micrograph; **b** map of tin; **c** map of titanium; and **d** map of silver

are formed at the joint. The tin and silver elements are still evenly distributed inside the solder. Especially for the silver, the diffusion behavior of silver to the bonding interface has not been observed.

In order to get more accurate and valuable data of the joint interface, TEM was used to obtain the relevant interface pictures. Figure 10 shows the TEM micrograph and element maps for SiC/SnAgTi joint soldered at 420 °C for 30 min, in which the maps of carbon, titanium, and silicon are shown in Fig. 10b–d, respectively. Just look at Fig. 10a, it is clear that there is new compound formed at the interface, although it does not present a continuous distribution. Moreover, combining with the distribution of active element titanium in Fig. 10c and the interface microstructure in Fig. 10a, it could be inferred that some potential new phases formed at the interface should contain titanium element. Besides, it can be found from Fig. 10b that the concentration of C was relatively high in a small area at the interface where new substance is possibly formed. However, the apparent diffusion behavior of silicon element could not be determined from Fig. 10d.

Figure 11 shows the EDS spectrum at the point marked in Fig. 10a. From the proportion data of each element, it can be seen that the relative titanium concentration of 17.81 wt% at the interface is obviously higher than the content of titanium in the solder. Meanwhile, the relative carbon concentration of 68.08 at.% at the interface is also obviously higher than the content of carbon in the SiC. These may preliminarily infer that at least titanium and carbon are involved in the formation of a Ti–rich or a C-rich substance at the interface.

3.3 The reactants at the interface

To confirm the interfacial reaction phases formed in the soldered joints, the interfacial microstructures had been investigated by TEM. Figure 12 is the TEM micrograph of cross-sectional view of SiC/Sn3.5Ag5Ti joint soldered at 250 °C for 60 min. The results show that the interface between SiC and active solder is very clean and the reactant is not detected at the interface. In a word, from the analysis of experimental data of SiC/Sn3.5Ag5Ti/SiC joints soldered at 250 °C, only titanium element was found to be
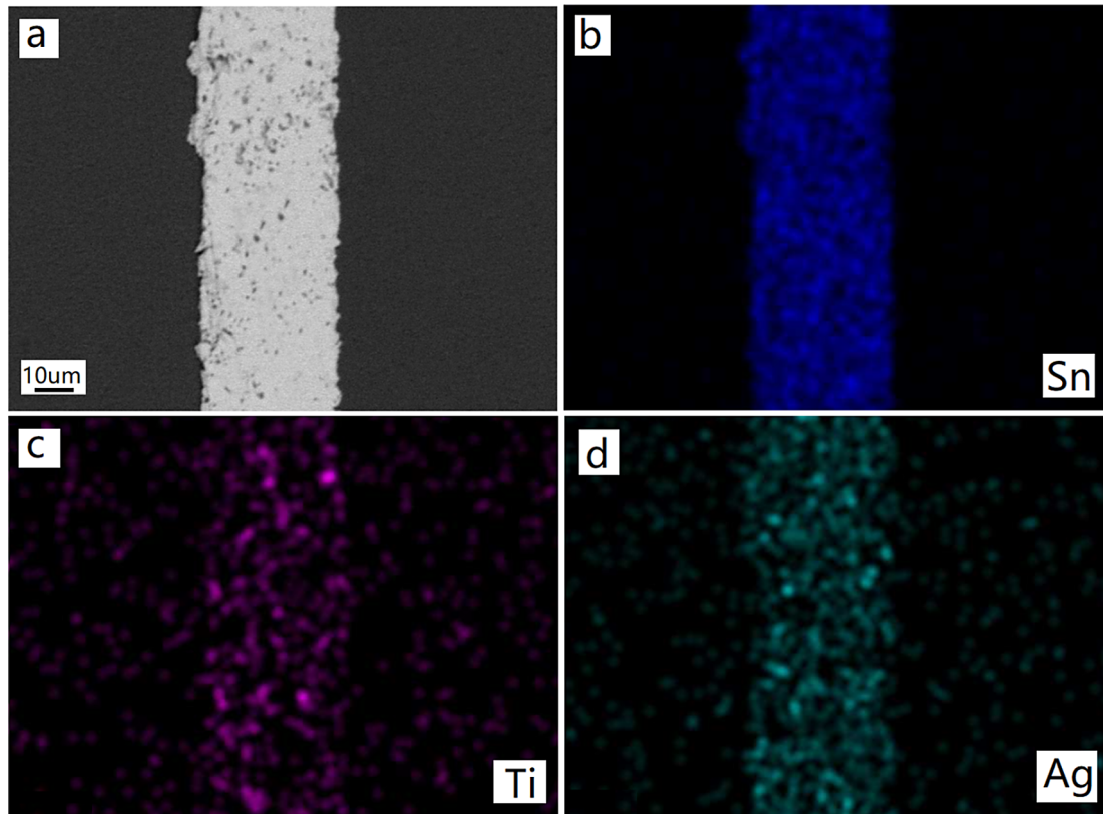
Fig. 7 Micrograph and element maps for SiC/SnAgTi/SiC joint soldered at 420 °C for 1 min. **a** micrograph; **b** map of tin; **c** map of titanium; **and d** map of silver

adsorbed at the joint interface, but chemical reaction product was not observed.

TEM micrographs of cross-sectional view of SiC/SnAgTi joint soldered at 420 °C for 30 min are shown in Fig. 13. It is obvious that there are some new compounds formed at the interface, as shown in Fig. 13a. To characterize the new compounds, the high-resolution transmission electron microscopy (HRTEM) of the marked area "Z1" and "Z2" were taken, as shown in Fig. 13b and c. Figure 13b reveals that the crystalline interplanar spacing is about 1.93 Å, 3.06 Å, and 1.93 Å, respectively, in three different lattice faces. The analysis result determined by HRTEM image has better tally with that of TiC, which is consistent with the lattice spacing of TiC (1 2 0), TiC (− 1 1 0), and TiC (− 2 − 1 0), respectively. To further confirm the phase of the "Z1" area, the best way is to take diffraction images. However, as the area is too small and compounds formed at the interface are quite brittle, it is quite hard to get diffraction images directly by TEM. So an indirect way performed by Gatan digital micrograph was tried to determine the phase of the "Z1" area, and the

diffraction pattern was built as shown in Fig. 13d. The result shows that the diffraction image of "Z1" area coincided with that of TiC, which could further illustrate that the compound formed at Z1 area is the TiC. Meanwhile, the "Z2" area was analyzed by the same method as above. The analysis result from Fig. 13c reveals that the crystalline interplanar spacing is about 2.12 Å, 1.77 Å, and 3.23 Å, respectively, in three different lattice faces. Among all possible Ti–Si phases, the crystalline interplanar spacing determined by HRTEM image has better tally with that of Ti_5Si_3, which is consistent with the lattice spacing of Ti_5Si_3 (− 2 1 − 2), Ti_5Si_3 (− 2 − 1 − 2), and Ti_5Si_3 (0 − 2 0), respectively. Besides, the diffraction image of "Z2" area was also obtained by Fourier transform method, as shown in Fig. 13e, which coincided with that of Ti_5Si_3. Therefore, it could further illustrate that the compound formed at Z2 area is Ti_5Si_3 most possibly.

In order to analyze the interfacial microstructure more completely, another part of the joining interface was analyzed simultaneously, as shown in Fig. 14. Among them, Fig. 14a is the microstructure of the
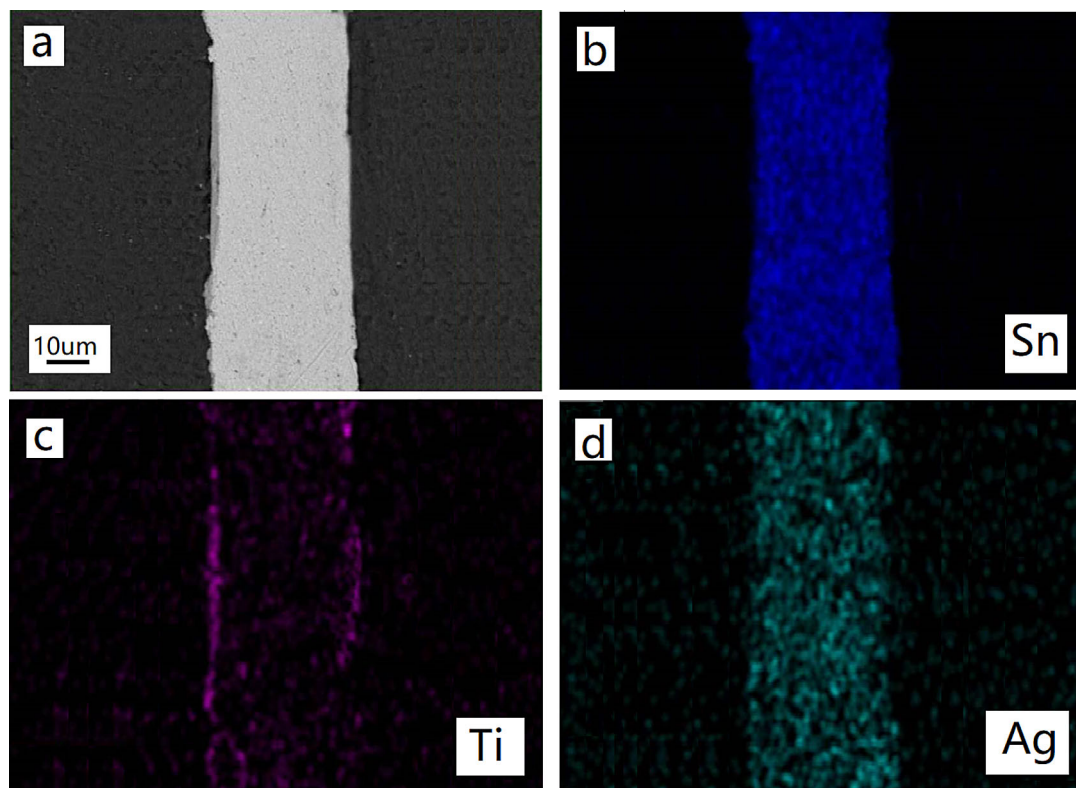
Fig. 8 Micrograph and element maps for SiC/SnAgTi/SiC joint soldered at 420 °C for 30 min. **a** micrograph; **b** map of tin; **c** map of titanium; **and d** map of silver

interface, Fig. 14b is the HRTEM image indicated in Fig. 14a and c is the diffraction pattern, respectively. The analysis result from Fig. 14b reveals that the crystalline interplanar spacing is about 1.60 Å, 1.95 Å, and 2.92 Å, respectively, in three different lattice faces. The analysis result determined by HRTEM image has better tally with $TiSi_2$, which is consistent with the lattice spacing of $TiSi_2$ (0 1 3), $TiSi_2$ (1 1 2), and $TiSi_2$ (− 1 0 1), respectively. Besides, the diffraction image of the marked area also coincided with that of $TiSi_2$. Hence it could further indicate that the new phase formed at the marked area in Fig. 14a is $TiSi_2$ most possibly. Thus, based on all above analysis, it could be inferred that there might be at least TiC, Ti_5Si_3, and $TiSi_2$ that formed discontinuously at the interface of SiC/SnAgTi joints.

4 Analysis and discussion

4.1 Diffusion of active Ti

By comparing the Ti segregation at the interface under two soldering temperatures, it can be found that the holding time required for the obvious segregation of titanium at the interface is different. So it should be interesting to analyze the diffusion behavior of titanium during soldering. For liquid, due to the regular arrangement of atoms disrupted, the atoms do Brown motion according to Langevin's law of motion [20]. In this case, the diffusing atoms are resisted by the neighboring atoms. The diffusion coefficient D can be given by the equation of Stokes–Einstein as follows:

$$D_{AB} = \frac{kT}{6\pi\mu_B r_A} \tag{1}$$

where the subscripts A and B represent the solute and solvent, respectively. μ_B is the viscosity of solvent, r_A is the radius of the solute atom, which is assumed to be spherical. k is the Boltzmann constant, and T is the temperature. The equation of Stokes–Einstein suggests that the diffusion coefficient D_{AB} is affected by the temperature T and viscosity μ_B. The diffusion coefficient is directly proportional to the temperature and inversely proportional to the viscosity.

However, this relationship only holds when the radius ratio of solute to solvent is greater than 5. In
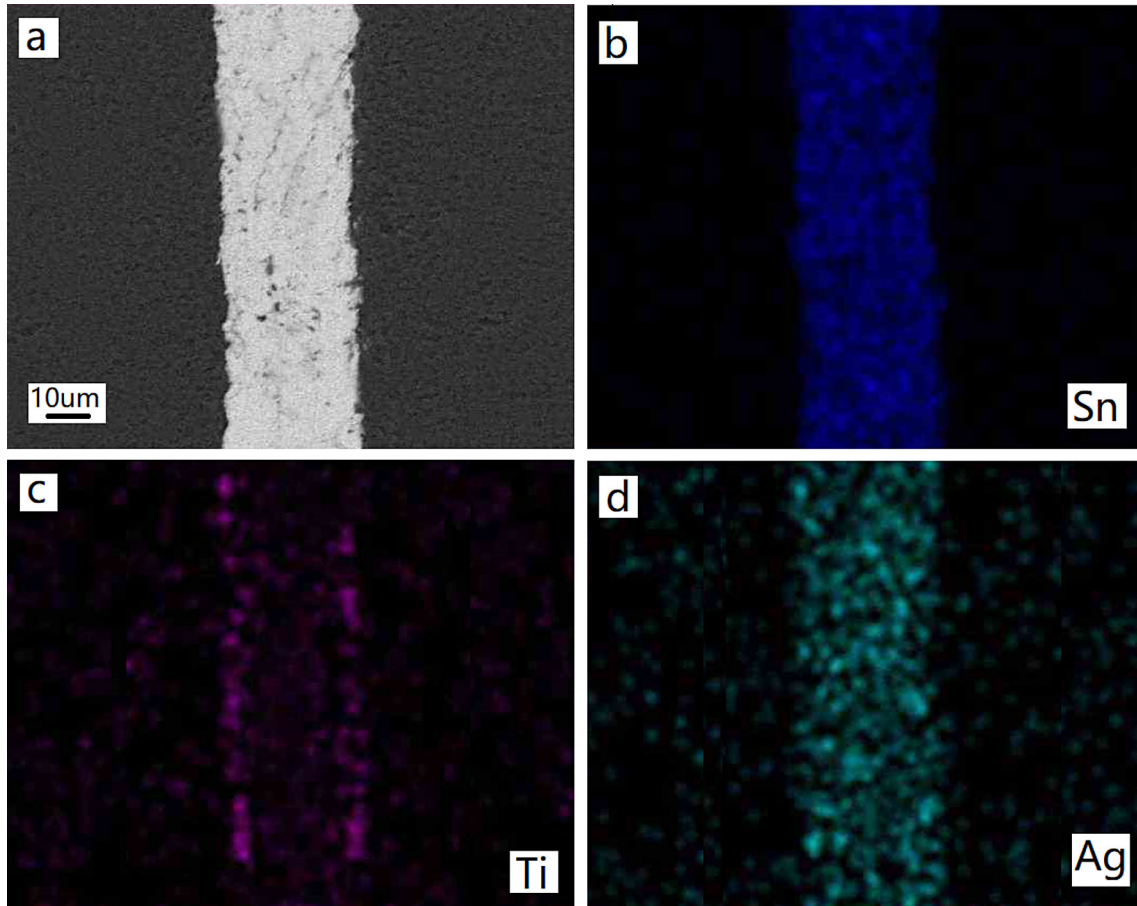
Fig. 9 Micrograph and element maps for SiC/SnAgTi/SiC joint soldered at 420 °C for 60 min. **a** micrograph; **b** map of tin; **c** map of titanium; **and d** map of silver

our material system, the radius of titanium atom is about 146 pm and that of Tin atom is about 140 pm, which is obviously not in conformity with the above requirements. Sutherland modified the Stokes–Einstein equation according to the theory of fluid dynamics [21], taking into account that the radius of solute atom is equal to that of solvent atom. When the radius of solute atom is equal to that of solvent atom, the Stokes–Einstein equation had been modified as follows:

$$D_{AB} = \frac{kT}{4\pi\mu_B r_A} \tag{2}$$

Obviously, this modified formula is more in line with our material system. Besides, considering the relationship between viscosity and temperature of molten metal, although many models or formulas have been put forward, the Arrhenius formula is the most commonly accepted [22], listed as follows:

$$\mu = A\exp\left(\frac{\varepsilon}{kT}\right), \quad A = \frac{h}{\upsilon_m} \tag{3}$$

where h is the Planck constant, υ_m is the size of a stream (ion, atom, or cluster), ε is the activation energy required for the flow mass to move from one equilibrium position to another. k is the Boltzmann constant, and T is the temperature.

Substitute formula (3) into formula (1), the diffusion coefficient can be rearranged as follows:

$$D_{AB} = \frac{kT}{4\pi A r_A}\exp\left(1 - \frac{\varepsilon}{kT}\right) \tag{4}$$

This shows that the relationship between diffusion coefficient and soldered temperature is exponential dependent. When the soldering temperature is increased, the active element Ti will diffuse to the interface more quickly, and the segregation of titanium at interface is faster. This is consistent with the results observed in our experiment. Therefore, the

Fig. 10 TEM Micrograph and element maps for SiC/SnAgTi joint soldered at 420 °C for 30 min. **a** micrograph; **b** map of C; **c** map of Ti; **and d** map of Si
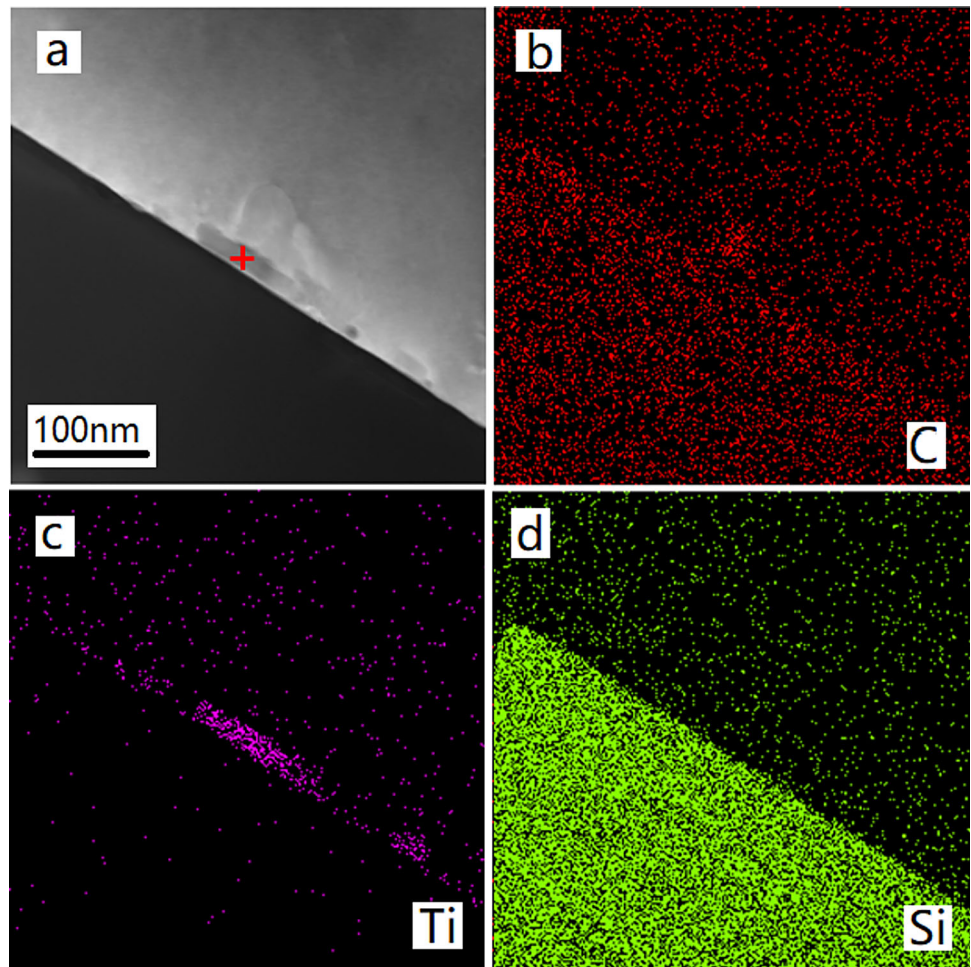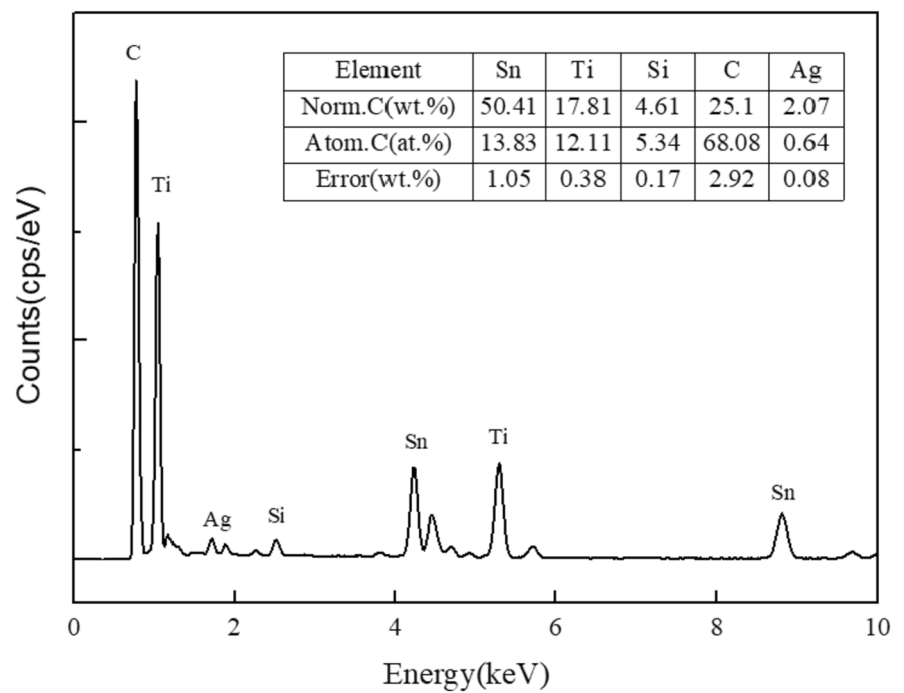

Fig. 11 EDS spectrum of the marked point as denoted in Fig. 8a

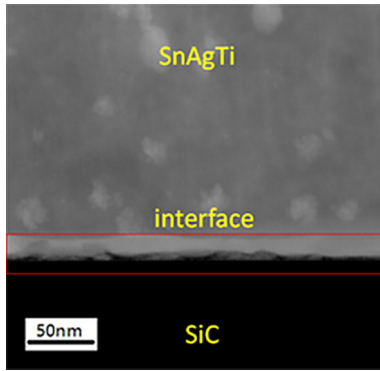| Element	Sn	Ti	Si	C	Ag
Norm.C(wt.%)	50.41	17.81	4.61	25.1	2.07
Atom.C(at.%)	13.83	12.11	5.34	68.08	0.64
Error(wt.%)	1.05	0.38	0.17	2.92	0.08

Fig. 12 TEM micrograph of cross-sectional view of SiC/SnAgTi joint soldered at 250 °C for 60 min

soldering temperature is a key factor which affects the diffusion behavior of titanium during soldering.

4.2 Active adsorption of Ti

In our material system, the adsorption of active element titanium at the bonding interface was observed concurrently at 250 °C and 420 °C when the soldering time is set long enough. In order to explore the reason of the phenomenon of adsorption and the mechanism of bonding, it is necessary to carry out some analysis. Firstly, when the solder is heated to the molten state, there is a repulsive force between the dissolved active atoms and tin atoms. Presumably, due to this repulsive force, some of the titanium atoms may be squeezed out onto the liquid surface and the solid–liquid interface, while some may return to the interface of clustered particles. Based on the above analysis, through a long distant migration, the last active elements will have two existing status: occupy the liquid surface and solid–liquid interface, and cluster inside of the liquid. If the attractive force of the solid surface to the active atom is stronger than that of the liquid body, the active atom would remain on the interface [18]. Secondly, the schematic crystal structure of 4H-SiC is shown in Fig. 15 [23]. From Fig. 15, it can be seen that the 4H-SiC consists of four Si–C diatomic layers arranged in the form of ABCB, which are stacked repeatedly along the (0001) direction. In our experiment, the surface (0001) of 4H-SiC is used as the soldering surface, which is a polar surface and contains Si surface with unsaturated chemical bond. There are Si suspension bonds, high energy, and unstable, easy to form adsorption with active metals [24]. When active Ti atoms reach the surface (0001) of 4H-SiC, the Ti atoms and Si atoms on the surface of 4H-SiC can share electrons to form covalent bonds [25], which makes the interfacial bonding succeed. Because the diffusion of active Ti is a slow process, it needs to take some time to form obvious segregation.

According to our previous research on the adsorption behavior of active element Ti on the
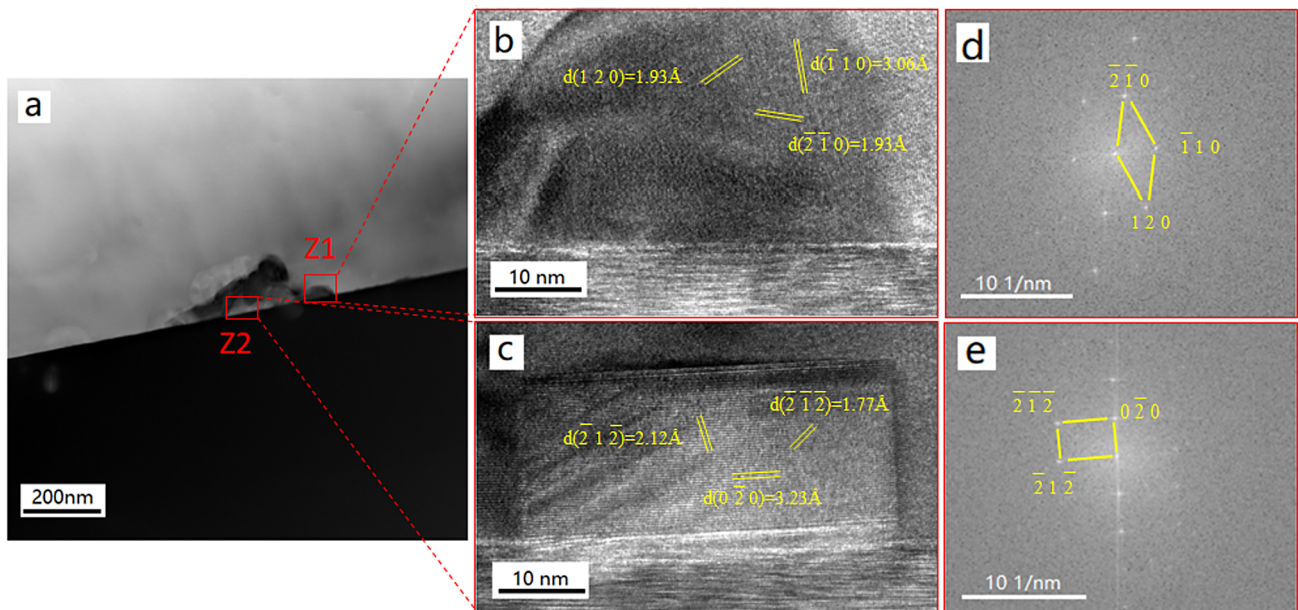

Fig. 13 TEM micrographs of cross-sectional view of SiC/SnAgTi joint soldered at 420 °C for 30 min. **a** Microstructure of the reaction layer; **b**, **c** HRTEM image indicated in Fig. 8a; **d**, **e** diffraction pattern
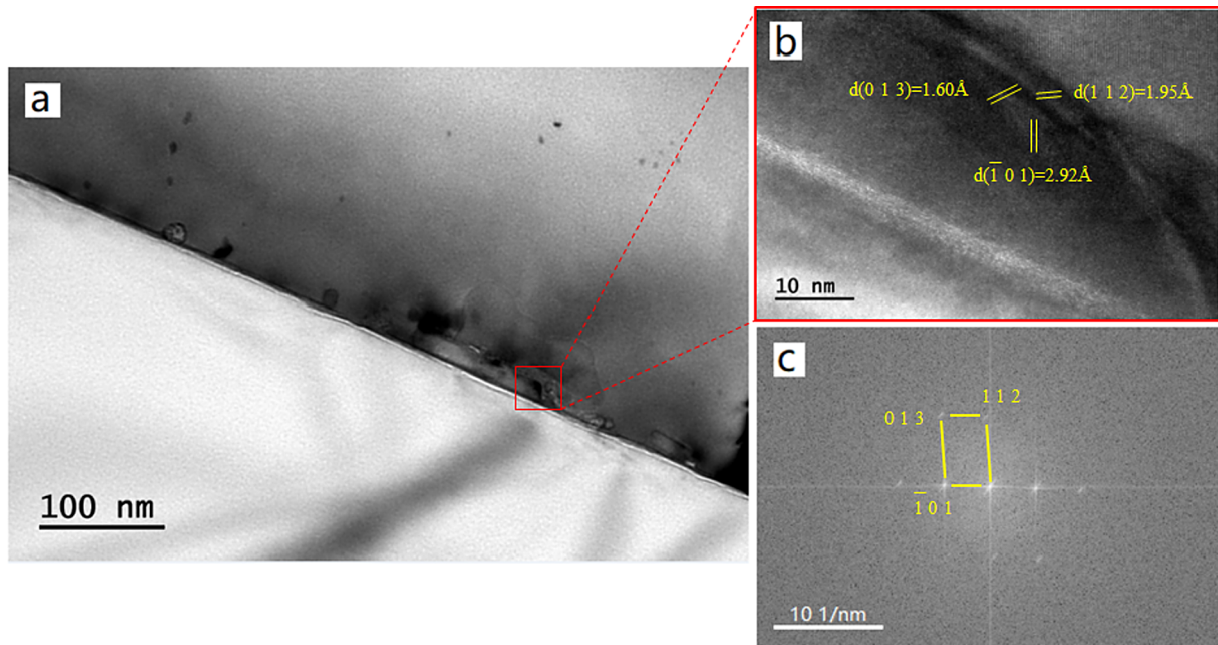
Fig. 14 TEM micrographs of cross-sectional view of SiC/SnAgTi joint soldered at 420 °C for 30 min. **a** Microstructure of the reaction layer; **b** HRTEM image indicated in Fig. 9a; and **c** diffraction pattern
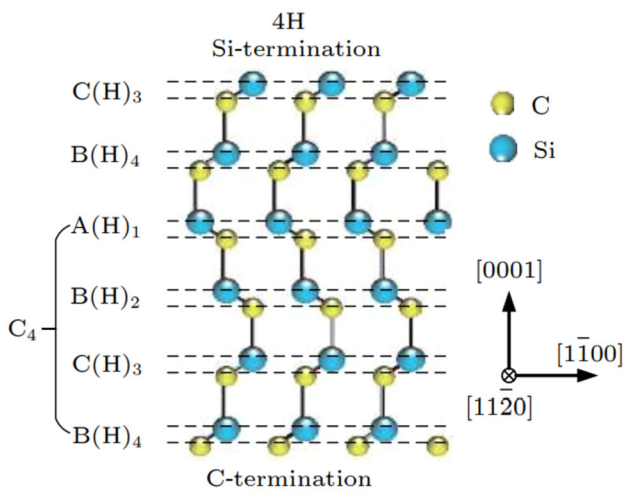
Fig. 15 Schematic crystal structure of 4H-SiC [22]

ceramic surface and the adsorption force calculation by Li [26, 27], the work of adhesion W could be obtained by the following formula:

$$W = S_W \times n_{ws} \tag{5}$$

where S_W is the slope parameter of the work of adhesion, which is related to the band gap of the ceramic. n_{ws} is the electron density at the boundary of the Wigner–Seitz cell of the metals. The S_W of SiC is about 500 mJ/m²/du, and n_{ws} of Ti is 3.51 du [27, 28]. The du is the density unit, and

$1\,du = 6 \times 10^{22}$ electrons/cm³. Therefore, when the titanium atoms arrive at the surface of silicon carbide, the work of adhesion of Ti on the surface of SiC could be calculated as follows:

$$W = 500\,\text{mJ/m}^2/\text{du} \times 3.51\,\text{du} = 1755\,\text{mJ/m}^2 \tag{6}$$

This shows that the adsorption force between active element titanium and silicon carbide does exist. And it is larger than that of active titanium on the surface of alumina and silicon dioxide in our previous studies [18, 29]. Owing to this adsorption force, when titanium atoms diffuse and reach at the interface, they are able to stay at the bonding interface and form segregation. In our preliminary studies, the adsorption phenomenon of active Ti on the surface of ceramics had been observed many times in different substrate materials, such as the surface of alumina on which no new phase was formed, and the surface of both silicon and silicon dioxide with reactant formation and etc. Consequently, it could be speculated that the adsorption between Ti and ceramic substrate is an important factor which contributes to the realization of bonding between Sn3.5Ag4Ti(Ce, Ga) and ceramic substrate when soldering at low temperatures. It also plays an important role in the bonding of Sn3.5Ag4Ti(Ce, Ga) and

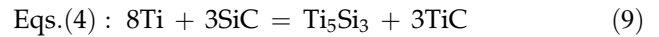SiC when soldered at 250 °C and 420 °C in these experiments.

4.3 Thermodynamics analysis

In order to understand the formation mechanism of interface products in the soldering process, it is necessary to deeply study and analyze the thermodynamics of soldering. Traditionally, the calculation formula of Gibbs free energy of standard reaction is a good way to analyze the chemical equilibrium of the reaction. According to the calculation of ΔG_T^θ, the possibility of spontaneous occurrence of chemical reaction between the active element Ti and silicon carbide could be assessed. In our material system, the possible chemical reactions between the active element Ti in the SnAgTi filler alloy and SiC substrate to form some compounds are in Fig. 16, in which 12 chemical reaction equations are involved. Moreover, the calculation results of ΔG_T^θ for each reaction at different soldering temperatures have been portrayed as curves, as shown in Fig. 16 as well [30].
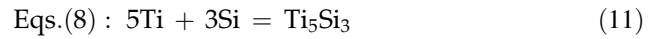
From graph 16, it can be seen that Eqs. (2), (4), and (8) have larger negative values, which means that these reactions are most likely to occur. The corresponding reaction equations are as follows:

$$\text{Eqs.(2)}: \quad 3Ti + 2SiC = TiSi_2 + 2TiC \tag{7}$$

$$\Delta G_T^\theta = -356.06 + 0.0136T \tag{8}$$

$$\text{Eqs.(4)}: \quad 8Ti + 3SiC = Ti_5Si_3 + 3TiC \tag{9}$$

$$\Delta G_T^\theta = -911.69 + 0.0008T \tag{10}$$

$$\text{Eqs.(8)}: \quad 5Ti + 3Si = Ti_5Si_3 \tag{11}$$

$$\Delta G_T^\theta = -579.07 - 0.0094T \tag{12}$$

Based on the above reaction equations, at 693 K, ΔG_T^θ of Eqs. (2), (4), and (8) are -346.635 kJ/mol, -911.136 kJ/mol, and -585.584 kJ/mol, respectively. The negative values of ΔG_T^θ signify that all these reactions could take place spontaneously. However, whether the reaction Eq. (8) occurs or not, it needs to take the occurrence of Eq. (3) as the precondition. The specific reaction of Eq. (3) is as follows;

$$\text{Eqs.(3)}: \quad Ti + SiC = TiC + Si \tag{13}$$
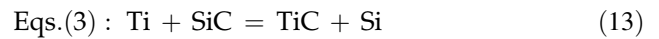
$$\Delta G_T^\theta = -110.88 + 0.0034T \tag{14}$$

When soldered at 693 K, ΔG_T^θ of Eq. (3) is -108.524 kJ/mol, which is higher than that of Eqs. (2), (4), and (8). Therefore, from the thermodynamic point of view, Eqs. (2) and (4) may be more likely to occur in the same soldering environment. The new substances Ti_5Si_3, TiC, and $TiSi_2$ which were
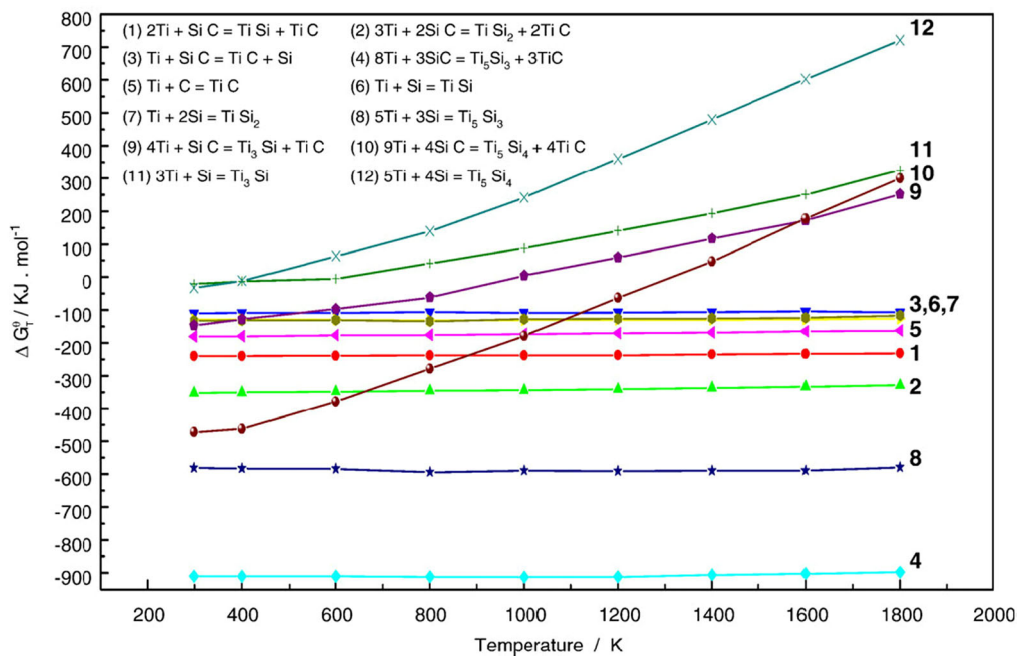

Fig. 16 ΔG_T^θ of the interfacial reaction between Ti and SiC at different temperatures [30]

found in the joint soldered at 693 K meet the formation conditions of the reaction thermodynamics. When the joints were soldered at 523 K, the ΔG_T^θ of Eqs. (2) and (4) at 523 K does not change much from that at 693 K, so these reactions also satisfy the thermodynamic conditions of spontaneous occurrence. However, the Gibbs value is the necessary and inadequate condition for the interface reaction. When it is less than zero, the reaction may occur spontaneously, but not always happens. Whether a reaction really happening remains to be depended on the dynamics of the reaction, which is related to the concentration, temperature of the reaction and etc. When soldered at 523 K in our material system, it maybe reacts spontaneously according to the thermodynamics, but its reaction rate might be too small to observe the reactants. This phenomenon is worth to study in the future and the mechanism could help researchers to well understand the processes of the active bonding.

4.4 Dynamic process of bonding

To well understand the low-temperature active bonding mechanisms between SiC and Sn3.5Ag4-Ti(Ce, Ga), it is necessary to explore the dynamic process of bonding, especially the behavior evolution of active element Ti in different stages of soldering process at two soldering temperatures. According to the previous analysis of diffusion behavior, the calculated adsorption force and interfacial thermodynamics analysis, and the bonding process under two different soldering temperatures, both can be divided into three stages, as shown in Fig. 17. Figure 17(a1), (b1), and (c1) demonstrate the behavior evolution of active element Ti when soldered at 250 °C. And Fig. 17(a2), (b2), and (c2) show the behavior evolution of active element Ti when soldered at 420 °C. The movement of an active atom in the molten active solder is actually a complex microprocess. First, in the initial stage of bonding, with innumerable collisions with other atoms, the active element Ti passes directly from the droplet to the interface by Brownian motion [18]. Second, due to the diffusion coefficient which is exponentially related to the bonding temperature, the active element Ti with bonding temperature of 420 °C will diffuse to the interface more quickly, and the segregation of titanium at interface is faster. Hence when the holding time reaches to be 30 min, a lot of active elements Ti with bonding

temperature of 420 °C have arrived at the interface and form segregation, a part of them involves in the reaction with SiC and forms new phases, while maybe only a small amount of Ti with bonding temperature of 250 °C has reached the interface and has not yet formed obvious segregation. Most of them are still doing directional diffusion. Third, with the prolongation of heat preservation time, more and more Ti atoms with bonding temperature of 250 °C arrived at the interface. They form obvious segregation at the interface when the holding time reaches to be 60 min. However, the Ti and SiC react spontaneously according to the thermodynamics, but according to the dynamics of the reaction, maybe its reaction rate is too low to observe the reactants. So the interface seems to be very clean. At this moment, a part of the active element Ti segregates at the interface with bonding temperature of 420 °C diffuses back to the liquid solder due to the concentration gradient and another part of them continue to react with SiC, and the gains of the new phases formed at the interface gradually grow up.

4.5 Shear strength

In this study, the bonding strength of two group samples with bonding temperature of 250 °C and 420 °C was tested. The average shear strength was measured to be 13.05 MPa, 15.83 MPa, 16.25 MPa, and 19.83 MPa for the samples soldered at 250 °C with soldering time of 1 min, 15 min, 30 min, and 60 min, respectively. The average shear strength of samples soldered at 420 °C with soldering time of 1 min, 15 min, 30 min, and 60 min was measured to be 16.82 MPa, 21.76 MPa, 23.17 MPa, and 25.62 MPa, respectively. The relationship between shear strength of the joints and soldering time at temperature of 250 °C and 420 °C is shown in Fig. 18. It can be seen intuitively that the shear strength for the samples soldered at 420 °C is higher than that of 250 °C. Moreover, with the increase of soldering time, the shear strength at both soldering temperatures presents an increasing trend. This may indicate that both of the soldering temperature and soldering time are important factors to affect the shear strength of the joints. Especially, the soldering temperature not only affects the diffusion behavior of titanium during soldering, but also directly affects if there are obvious new phases formed at the interface. From another point of view, the formation of the reaction product
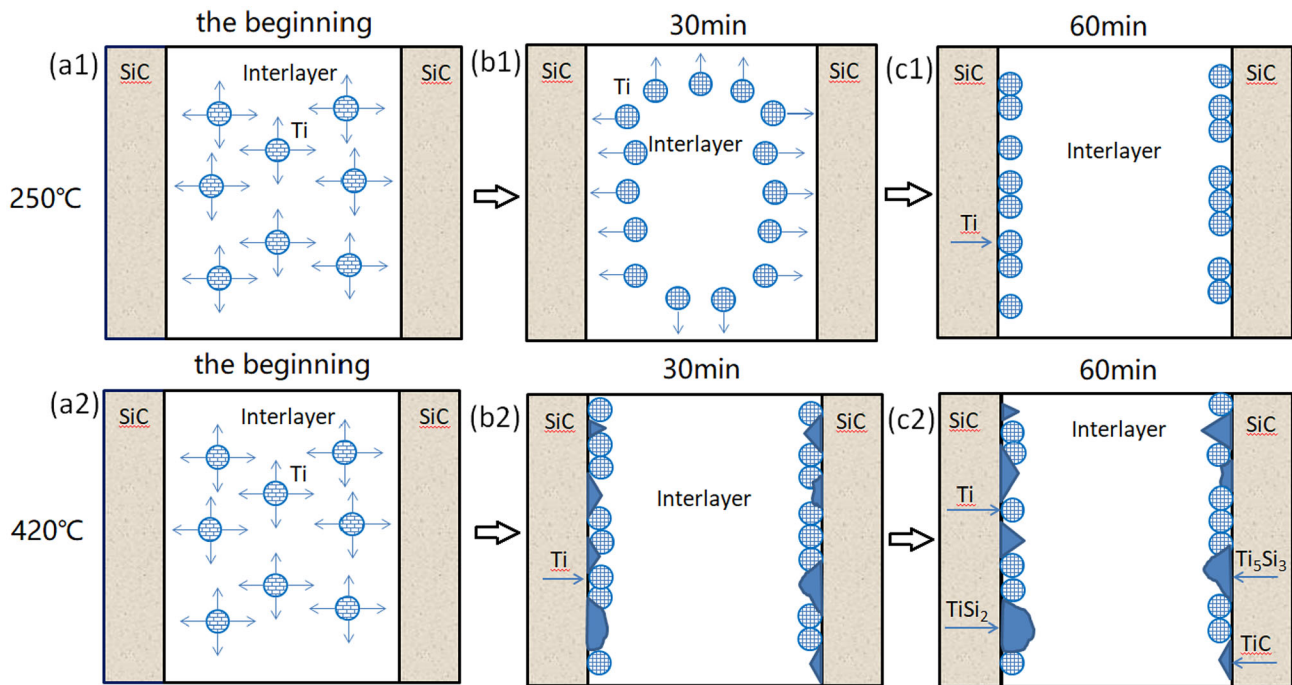
Fig. 17 Evolution behavior of active element Ti in different stages of soldering process at two soldering temperatures (a1) migration of Ti atoms (b1) directional diffusion of Ti (c1) titanium adsorption stage (a2) migration of Ti atoms (b2) titanium adsorption and interfacial reaction stage (c2) interfacial materials continues to form stage
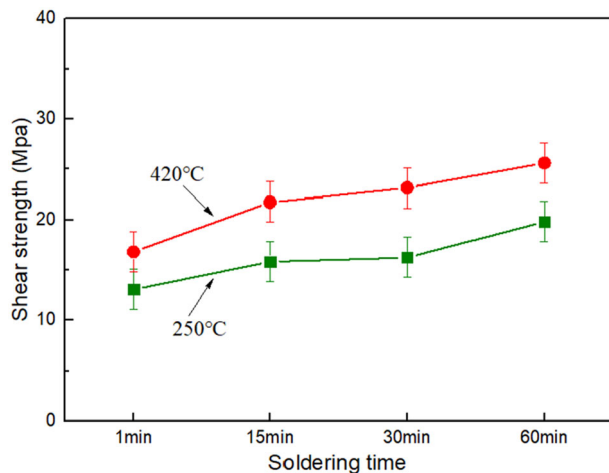

Fig. 18 Shear strength of the joints vs soldering time at temperature of 250 °C and 420 °C

plays a critical role to obtain more reliable bond between the silicon carbide and SnAgTi, although it is not a necessary condition to realize bonding. The shear strength meets the requirements of die bonding application in American military standards <MIL-STD883G-2006 Test standard of microelectronic device>, but since we have not done the aging test of the SiC–SiC joint at standard aging temperature, the specific scope of application temperature for the Si/Sn3.5Ag4Ti(Ce,Ga)/Si remains to be determined.

5 Conclusions

To well understand the low-temperature active bonding mechanisms and explore if the formation of new phases at the interface is a necessary condition for the interfacial connection bonding between SiC and Sn3.5Ag4Ti(Ce,Ga), this paper carried out the research on the low-temperature active bonding of SiC using Sn3.5Ag4Ti(Ce,Ga) solder filler at bonding temperature of 250 °C and 420 °C, respectively. The microstructure of the interface, the elemental distribution, and the new compound formed at the interface were characterized. The shear strength of the joints with different bonding temperatures and holding time was tested. The main conclusions are summarized as follows:

1. For SiC/Sn3.5Ag4Ti(Ce,Ga)/SiC joints soldered at 250 °C, as the diffusion rate is relatively lower than that at 420 °C, only a small amount of Ti has reached the interface and not yet formed obvious segregation at the initial stage of soldering.

Obvious segregation has been found at the interface when the holding time is extended to be 60 min. The results of TEM analysis show that the interface of SiC/Sn3.5Ag5Ti(Ce,Ga) joint soldered at 250 °C for 60 min is very clean and the reactant is not observed at the interface. The bonding mechanism might be that the Ti atoms arrived at the interface and Si atoms on the surface(0001) of 4H-SiC can share electrons to form covalent bonds, which makes the interfacial bonding succeed.

2. For SiC/Sn3.5Ag4Ti(Ce,Ga)/SiC joints soldered at 420 °C, the Ti element has obviously segregated at the interface when the holding time is set to be 30 min and 60 min. However, there is still no obvious segregation of Ti found at the interface with holding time of 1 min. It may be because although the diffusion rate is relatively higher than that at 250 °C, it also needs to take time to form obvious segregation. Based on the careful analysis of the TEM data, it confirmed that there might be at least TiC, Ti_5Si_3, and $TiSi_2$ formed discontinuously at the interface of SiC/SnAgTi joints soldered at 420 °C for 30 min, which meets the formation conditions of the reaction thermodynamics.

3. The evolution behavior of active element Ti in soldering process was analyzed and the bonding process under two soldering temperatures can be divided into three stages. First, in the initial stage of bonding, the active element Ti diffuses directly from the droplet to the interface by Brownian motion. Second, due to the diffusion coefficient, it is exponentially related to the bonding temperature, when the holding time reaches to be 30 min, a lot of active elements Ti with bonding temperature of 420 °C have arrived at the interface and formed segregation, a part of them involves in the reaction with SiC to form new phases. For the soldering temperature of 250 °C, only a small amount of Ti has reached the interface and has not yet formed obvious segregation for the soldering time of 30 min. Third, with the prolongation of heat preservation time, more and more Ti atoms with bonding temperature of 250 °C arrive at the interface and form obviously segregation. For the bonding temperature of 420 °C, a part of the active element Ti segregated at the interface may diffuse back to the liquid solder due to the concentration gradient and another part of them continue to react with SiC, and the grains of the new phases formed at the interface gradually grow up.

4. The work of adhesion of Ti on the surface of SiC is calculated to be 1755 mJ/m^2. This shows that the adsorption force between active element titanium and silicon carbide does exist. It might be inferred that the joining could be accomplished by chemical adsorption of titanium on the silicon carbide/solder interface, regardless of whether an interfacial reaction layer is formed or not. This could explain that the formation of interface compound might be not a necessary condition for interface connection.

5. The average shear strength is measured to be 13.05 MPa, 15.83 MPa, 16.25 MPa, and 19.83 MPa for the samples soldered at 250 °C with soldering time of 1 min, 15 min, 30 min, and 60 min, respectively, while the average shear strength of samples soldered at 420 °C with soldering time of 1 min, 15 min, 30 min, and 60 min is measured to be 16.82 MPa, 21.76 MPa, 23.17 MPa, and 25.62 MPa, respectively. The shear strength for the samples soldered at 420 °C is higher than that of 250 °C. This may show that the formation of the reaction products plays a critical role to obtain more reliable bond between the silicon carbide and SnAgTi, although it might be not a necessary condition to realize bonding.

Author contributions

All authors contributed to the study conception and design. Material preparation, data collection, and analysis were performed by LXC, KBM, XJY, and ZLL. The first draft of the manuscript was written by LXC and GYL, and all authors commented on previous versions of the manuscript. All authors read and approved the final manuscript.

Data availability

The data that support the finding of this study are available from the corresponding author upon reasonable request.

Code availability

Not applicable.

Declarations

Conflict of interest No conflict of interest exits in the submission of this manuscript, and manuscript is approved by all authors and the responsible authorities at the institute for publication.

References

1. L. Wu, L. Zhu, W. Guo, S. Sun, W. Niu, J. Xue, J. Zhai, H. Ma, R. Lin, H. Lin, K. Plucknett, Y. Liao, T. Liu, Q. Ren, J. Eur. Ceram. Soc. **41**, 225–232 (2021)
2. X. Song, Z. Chen, S. Hu, X. Duan, Y. Lei, C. Niu, J. Feng, J. Am. Ceram. Soc. **103**, 912–920 (2019)
3. F. Mu, Y. Wang, R. He, T. Suga, Materialia **3**, 12–14 (2018)
4. G. Lyu, Y. Wang, J. Wei, Z. Zheng, J. Sun, L. Zhang, K.J. Chen, IEEE T. Power Electron. **35**, 9669–9679 (2020)
5. Y. Feng, H. Sun, X. Yang, K. Liu, J. Zhang, J. Shen, D. Liu, Z. Cai, F. Xu, N. Tang, T. Yu, X. Wang, W. Ge, B. Shen, Appl. Phys. Lett. **118**, 052104 (2021)
6. X. Dai, J. Cao, Z. Chen, X. Song, J. Feng, Ceram. Int. **42**, 6319–6328 (2016)
7. X. Dai, J. Cao, Y. Tian, Z. Chen, X. Song, J. Feng, Mater. Charact. **118**, 294–301 (2016)
8. M. Singh, R. Asthana, N. Sobczak, J. Mater. Eng. Perform. **29**, 4898–4912 (2020)
9. M. Li, X. Song, S. Hu, Z. Chen, Y. Song, C. Niu, J. Am. Ceram. Soc. **102**, 3318–3328 (2019)
10. Z. Li, R. Wei, Q. Wen, Z. Zhong, K. Song, Y. Wu, Vacuum **173**, 109160 (2020)
11. B. Wu, X. Leng, Z. Xiu, J. Yan, Sci. Rep. (2018). https://doi.org/10.1038/s41598-018-34635-w
12. W. Yu, Y. Liu, X. Liu, Mater. Des. **150**, 9–16 (2018)
13. L.C. Tsao, S.Y. Chang, Y.C. Yu, Trans. Nonferr. Metal. Soc. **28**, 748–756 (2018)
14. S. Mishra, A. Sharma, D.H. Jung, J.P. Jung, Met. Mater. Int. **26**, 1087–1098 (2020)
15. Y.S. Chung, T. Iseki, Eng. Fract. Mech. **40**, 941–949 (1991)
16. L. Gremillard, E. Saiz, V.R. Radmilovic, A.P. Tomsia, J. Mater. Res. **21**, 3222–3233 (2006)
17. C. Rado, S. Kalogeropoulou, N. Eustathopoulos, Mater. Sci. Eng. A **276**, 195–202 (2000)
18. L.X. Cheng, G.Y. Li, Z.L. Li, Z.Z. Wu, B. Zhou, J. Mater. Sci. Mater. Electron. **26**, 6004–6012 (2015)
19. A.K. Niessen, F.R. de Boer, R. Boom, P.F. de Chatel, Calphad **7**, 51–70 (1983)
20. H. Yang, Doctoral Dissertation of Xiangtan University (2010)
21. W. Sutherland, IDEA Fit. J. **9**, 781–785 (1905)
22. Z.X. Yang, H.R. Geng, Z.D. Tao, C.J. Sun, J. Atomic Mol. Phys. **21**, 663–666 (2004)
23. L. Yuan, S. Ai-Hong, C. Guo-Yu, G. Bing-Dong, Acta Phys. Sin. **68**, 268–275 (2019)
24. Y. Li, Master's Dissertation of Jiangsu University (2017)
25. Q.L. Zhang, *Inorganic Chemistry Series vol. 8, Titanium, vanadium, Chromium Group*, 1st edn. (Science Press, Beijing, 1998)
26. J.G. Li, Mater. Lett. **22**, 169–174 (1995)
27. J.G. Li, Mater. Chem. Phys. **47**, 126–145 (1997)
28. B.W. Zhang, W.Y. Hu, X.L. Shu, *Theory of Embedded Atom Method and its Application to Materials Science*, 1st edn. (Hunan University Press, Changsha, 2003)
29. L.X. Cheng, M.R. Liu, X.Q. Wang, B.H. Yan, G.Y. Li, Mater. Sci. Eng. A **680**, 317–323 (2017)
30. J. Li, L. Liu, Y. Wu, W. Zhang, W. Hu, Mater. Lett. **62**, 3135–3138 (2008)